Received: 17 May 2022 | Revised: 26 July 2022 | Accepted: 24 August 2022

DOI: 10.1002/lio2.917

ORIGINAL RESEARCH

Laryngoscope Investigative Otolaryngology

Circulatory disturbance of the cochlear spiral modiolar artery in a type 2 diabetic mouse model

Young Joon Seo MD, PhD[1,2,3] | Dae Bo Shim PhD[4] | Arazu Sharif[5] | Zeke Samson[3] | Ryu Takechi PhD[5] | Daniel Brown PhD[3]

[1]Department of Otorhinolaryngology, Yonsei University Wonju College of Medicine, Wonju, South Korea

[2]Research Institute of Hearing Enhancement, Yonsei University Wonju College of Medicine, Wonju, South Korea

[3]Faculty of Health sciences, Curtin University, Bentley, WA, Australia

[4]Department of Otorhinolaryngology, Myongji Hospital, Hanyang University College of Medicine

[5]Curtin Health Innovation Research Institute, Curtin University, Bentley, WA, Australia

Correspondence
Daniel Brown, School of Pharmacy and Biomedical Sciences, Curtin University, Building 102, Curtin Perth, Kent Street, Bentley, Western Australia 6102, Australia.
Email: daniel.brown2@curtin.edu.au

Abstract

Objective: This study aimed to identify significant differences in cochlea microvessel size between a diabetic mouse model (db/db) and normal mice using three-dimensional (3D) quantitative analysis.

Methods: Six control heterozygote db/+ as well as 18 male B6/BKS(D)-Lepr^{db}/J (db/db) mice aged 14 ($n = 9$) and 28 ($n = 9$) weeks were examined. After clearing the cochlea, we reconstructed the 3D volumes of the spiral modiolar artery (SMA) in the cochlea using light-sheet microscopy and analyzed vessel wall thickness, cross-sectional area, short and long diameter, and vessel height.

Results: The average SMA-wall thickness in the db/db-mouse group (3.418 ± 0.328 μm) was greater than that in the control group (2.388 ± 0.411 μm). The average cross-sectional outer area, short diameter, and long diameter of the SMA in db/db mice were significantly larger than those in control mice (all $p < 0.001$). The cross-sectional areas increased with age (control: 221.782 ± 121.230 μm, 14 weeks; 294.378 ± 151.008 μm, and 28 weeks; 312.925 ± 147.943 μm).

Conclusion: The db/db mice had thicker and larger proximal-SMA vessel walls and diameters than control mice, respectively, thus potentially inducing increased blood viscosity or vascular insufficiency and aggravating hearing loss in type 2 diabetes mellitus.

Level of Evidence: IIb

KEYWORDS

db/db mice, diabetes mellitus, hearing loss, light sheet microscopy, spiral modiolar artery

1 | INTRODUCTION

Although several hearing-loss etiologies have been proposed, including viral infection, vascular disturbance, and immune-mediated mechanisms, the causes of inner-ear disorders, including sudden sensorineural hearing loss, noise-induced hearing loss, Meniere's disease, and presbycusis, are unclear.[1] Several studies have investigated inner-ear disorders and impaired cochlear blood flow in animal models. Abnormal cochlear microcirculation has long been considered a crucial cause of noise-induced hearing loss.[2] Animal models of cochlear microcirculation have provided a decent understanding of diseases associated with cochlear blood supply dysfunction, thus directly addressing vascular-related hearing disorders.[3]

This is an open access article under the terms of the Creative Commons Attribution-NonCommercial-NoDerivs License, which permits use and distribution in any medium, provided the original work is properly cited, the use is non-commercial and no modifications or adaptations are made.
© 2022 The Authors. *Laryngoscope Investigative Otolaryngology* published by Wiley Periodicals LLC on behalf of The Triological Society.

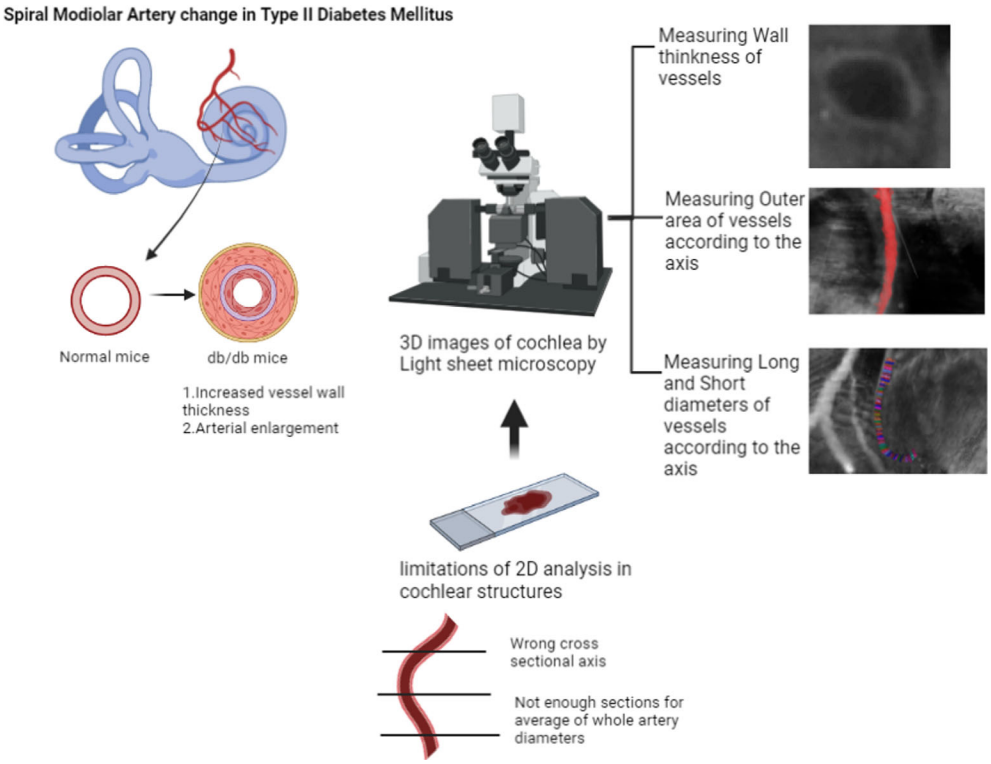

FIGURE 1 Three-dimensional analysis of the spiral modiolar artery (SMA) in the cochlea. The scheme reveals that db/db mice exhibited increased vessel-wall thickness and enlarged vessels of the SMA compared with those of normal mice.

Hearing loss is a common complication in patients with diabetes mellitus (DM).[4] However, the etiology and nature of hearing loss associated with DM remain controversial. DM is strongly associated with accelerated atherogenesis. Increased vessel-wall thickness has been reported in human temporal bones in DM, and periodic acid-Schiff-positive material has been detected in the vascular walls of the cochlea in patients with diabetes.[5] Kariya et al. demonstrated that type 2 diabetic human cadavers with insulin therapy exhibited increased vessel-wall thickness and vessel-wall ratio compared with patients with type 1 DM.[6] The cochlea in patients with DM is potentially related to circulatory disturbances compared with that in age-matched normal controls. However, the human study had limitations in terms of varying values of vessel thickness due to the limited number of subjects with available audiograms and postmortem examinations.

B6/BKS(D)-Lepr^{db}/J (db/db) mice are a perfect animal model of type 2 diabetes. The phenotypes of severe obesity, hyperphagia, polydipsia, and polyuria are caused by a spontaneous mutation in the leptin receptor. db/db mice were differentiated by spontaneous mutations in different sites of leptin receptors, and they exhibit abnormal metabolic, reproductive, and immune phenotypes.[7] A genetically diabetic db/db-mouse model of type 2 diabetes is characterized by nephropathy and neuropathy, but not retinopathy, during early examinations. Basement-membrane thickening and accumulation of basement-membrane material were observed in the outer plexiform layer capillaries of diabetic db/db-mice retinas. At 19 weeks, the mice exhibited significantly increased retinal vascular leakage and decreased levels of tight-junction proteins in the retina. Moreover, the expression of proinflammatory factors, such as ICAM-1 and TNFα, is drastically upregulated in diabetic retinas.[8]

In this study, we compared the vessel microstructure between a diabetic mouse model (db/db) and normal mice. Light-sheet fluorescence microscopy (LSFM) was used to obtain a highly resolved three-dimensional (3D) visualization of the spiral modiolar artery (SMA) in the inner ear (Figure 1). We considered LSFM a sensitive and reliable method for quantifying the complex architecture of microvessel networks in the inner ear.

2 | MATERIALS AND METHODS

2.1 | Mice

Eighteen male 5-week old B6/BKS(D)-Leprdb/J (db/db) mice (natural mutation resulting in leptin-receptor deficiency) aged and six control db/+ heterozygote mice were obtained from the Animal Resources Centre (Murdoch, Western Australia). Mice were provided with standard rodent maintenance chow (AIN-93M, Specialty Feeds, WA, Australia) and had ad libtium access to food and water. Animals were kept in groups of 2–4 in individually ventilated cages with 12 h light/dark cycle under ambient temperature of 22°C.

All animal procedures were approved by the Curtin Animal Ethics Committee (approval no. ARE2020-12) and performed in accordance with the Australian Code for the Care and Use of Animals for Scientific Purposes, 8th Edition.

The cochleae were harvested at 28 weeks in the control group and at 14 and 28 weeks in db/db mice. All mice were anesthetized with isoflurane. All mice were sacrificed by cervical dislocation, and both cochleae were promptly dissected. The cochleae were perfused

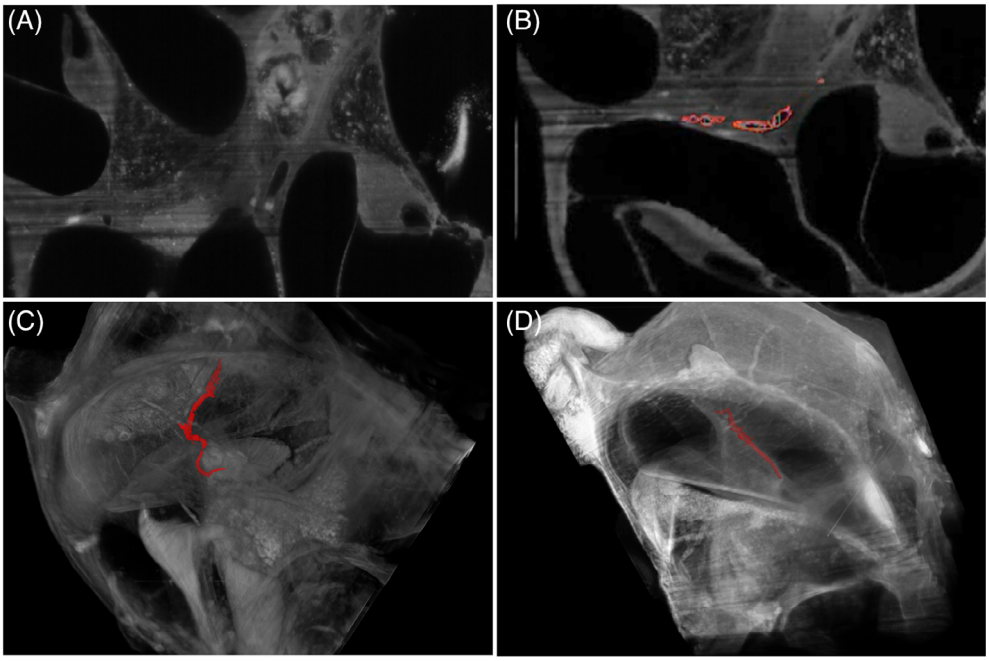

FIGURE 2 Vessel tracking and reconstruction from the binary mask of the blood-vessel compartment. (A) Original two-dimensional TIFF files were obtained from the light-sheet microscope. (B) Auto-Demarcating the SMA from the basal turn to middle turn in Arivis 4D software based on thresholds corresponding to their respective autofluorescence intensities. (C,D) Images for vessel reconstruction from the basal to the middle turn.

with a fixative containing 4% paraformaldehyde in phosphate-buffered saline (pH 7.4) at room temperature. The apical portion of the bony cochlea was gently opened to allow the fixative to perfuse through the tissues. The cochleae were decalcified by immersion in 10% ethylenediaminetetraacetic acid (National Diagnostics, Atlanta, GA) for 24 h. They were subsequently rinsed with Sorenson's buffer; dehydrated in a series of 50%, 75%, 90%, and 100% ethanol (8–12 h each step); and immersed in Spalteholz solution for 24 h to render the sample optically transparent. Thereafter, samples were imaged using a custom LSFM, based on the method described by Santi et al.,[9] where "virtual slices" of the inner ear were imaged at 5-mm steps in the axial plane, detailed in Brown et al.,[10] providing a "z-stack" of between 300 and 1000 virtual slice images.

2.2 | Imaging process and analysis

Image processing, segmentation, modeling, and analysis of microvascular networks were automated using a combination of readily available software tools to determine the length density of microvessels as a function of vessel diameter. LSFM z-stacks were analyzed using ImageJ software, with 3D volumes segmented for volume analysis using the Segmentation 3D plugin. Tag Image File Format (TIFF) files collected from the light-sheet microscope were reconstructed into representative 3D images. Following data reconstruction using Arivis vision4D (Germany) software, the fluorescence-intensity data of the cochlea was exported as a TIFF series. We tracked the SMA from the basal to the middle turn of the cochlea demarcated on each imported slide. SMA volumes were determined separately, based on thresholds corresponding to their respective autofluorescence intensities. Vessel-tracking and -extraction numerical data from the binary mask of the blood-vessel compartment were visually evaluated for matching with the original data (Figure 2).

We compared SMA characteristics using three parameters: (1) average vessel-wall thickness, (2) average cross-sectional area, and (3) short/long diameter and height of the sliced SMA.

After reconstructing the SMA volume, we calculated vessel-wall thickness in microns in the cross-sectional view (Figure 3). The average vessel-wall thickness and circumference length per vessel cross-section were determined using the following formula, with circumference length being measured manually in sectioned view:

$$\text{Average vessel} - \text{wall thickness} = (\text{outer area of vessel} - \text{inner area of vessel})/\text{circumference length}$$

To calculate the average cross-sectional area (outer area) of the SMA, we divided the SMA volume (Figure 4A) by the SMA length (Figure 4B).

The image was sectioned transversally using an ortho slicer tool, and a region of interest of 10 μm in thickness was selected. For a sliced object, we measured the short and long diameters in the horizontal sectional area and heights in the sagittal view of the sliced object (Figure 5).

2.3 | Statistical analysis

Variables were analyzed using parametric statistical methods, such as the independent *t* test, in the two groups. The data were compiled and presented as the frequency of vessel distribution and statistically analyzed using a one-way analysis of variance in the three groups. All variables were analyzed using SPSS Statistics for Windows (version 25.0; IBM Corporation, Armonk, NY). Statistical significance was set at $p < 0.05$.

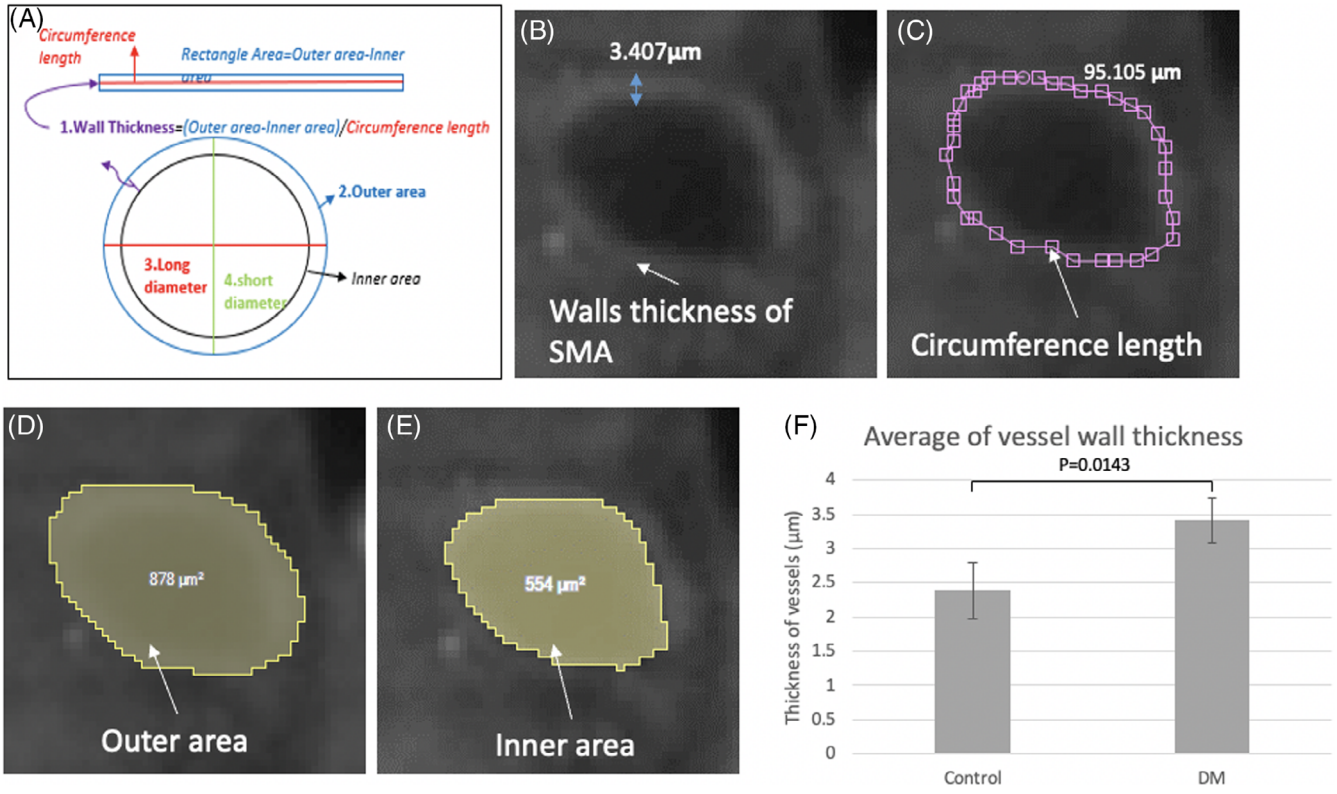

FIGURE 3 Measurement of SMA vessel-wall thickness in cross-sectioned images. (A) Definition and formula for calculating vessel-wall thickness. Examples of the measurement of (B) SMA wall thickness, (C) the circumference length according to the mid-layer of the vessel wall, (D) outer area of the vessel, and (E) inner area of the vessel. (F) Graph comparing the average vessel-wall thickness between the control and db/db-mice (DM) groups. The lengths of the bars and mean ± SEs of the values.

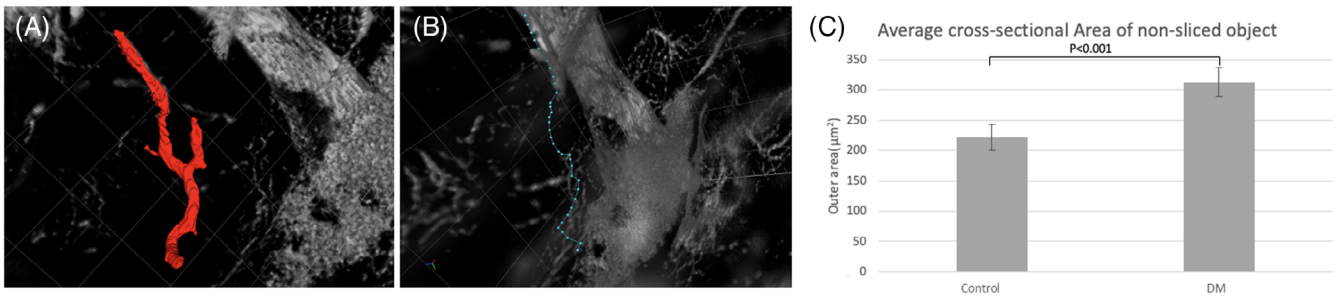

FIGURE 4 Measurement of SMA cross-sectional area in nonsliced objects. (A) Example of three-dimensional reconstructed SMA. (B) Tracing of SMA length; this could be manually traced using the polyline of each dot. (C) Graph comparing the average SMA cross-sectional area. The lengths of the bars and mean ± SEs of the values.

3 | RESULTS

3.1 | SMA vessel-wall thickness in cross-sectioned images

We calculated the long rectangular area of the vessel walls using the following formula: outer area—inner area of the vessel. Thereafter, we determined vessel-wall thickness after dividing the rectangular area by the circumference length of the mid-vessel wall in a single cross-sectional image (Figure 3A–E). The circumference was larger in the db/db-mice group (94.288 ± 11.132 μm) than that in the control group (89.918 ± 17.323 μm). The average SMA vessel-wall thickness in the db/db-mice group (3.418 ± 0.328 μm) was thicker than that in the control group (2.388 ± 0.411 μm) (Figure 3F). A significant difference was observed between the groups ($p = 0.0143$).

3.2 | SMA cross-sectional area in nonsliced objects

In the reconstructed volume of the SMAs, we calculated the average SMA cross-sectional area divided by SMA length, which could be traced manually using the polyline of each dot. The outer cross-

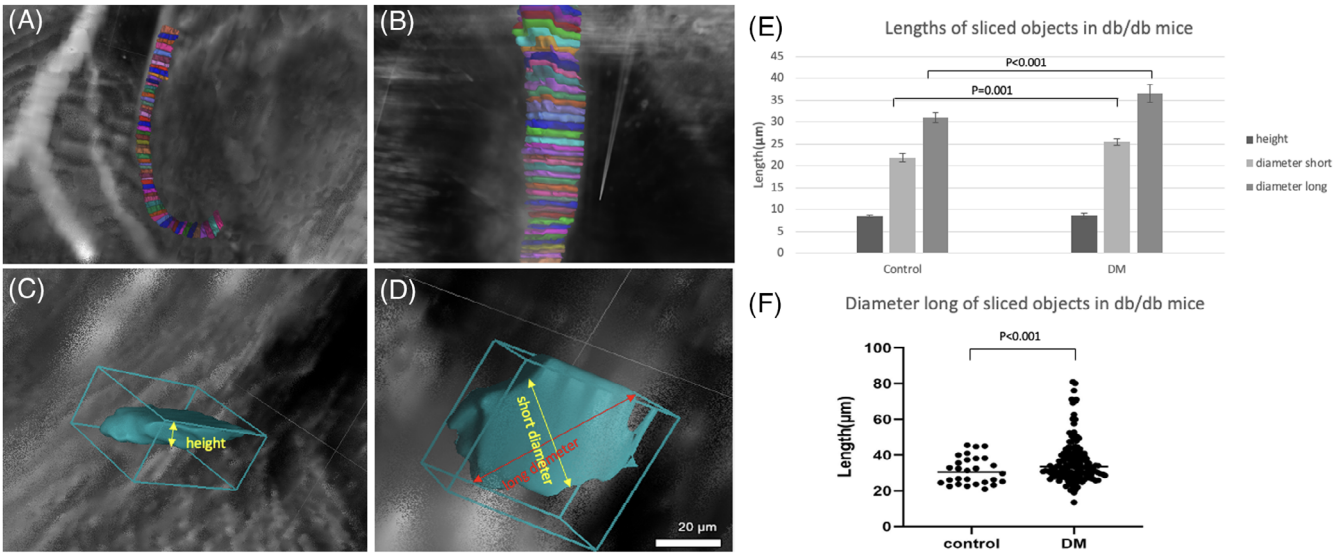

FIGURE 5 Measurement of SMA diameters in sliced objects. (A,B) Slicing with regular heights (approximately 8 μm) according to the longitudinal SMA length. (C) Measuring the height in a single slice. (D) Measuring the shortest and longest diameters in the horizontal plane of a single slice. (E) Graph comparing the lengths, short diameter, and long diameter of slices between the control and db/db mice (DM). (F) Graph with dot plots comparing the long diameter of slices in both groups showing distributions of each values. In the DM group, it showed up to 80 μm in the long diameter of sliced objects.

sectional area (SMA volume/SMA longitudinal length) was 221.782 ± 121.230 μm in the control group and 308.933 ± 179.977 μm in the db/db-mice group. The average cross-sectional outer area of the SMA in the db/db mice was significantly larger than that in the control mice ($p < 0.001$).

3.3 | SMA diameters in sliced objects

In Figure 5, we sliced the entire long SMA vertically to the length axis with a regular thickness (height). This revealed that the SMA diameters in db/db mice, including the short and long diameters, were longer than those in control mice. There were also significant differences in the short diameter between db/db (25.476 ± 4.913 μm) and control (21.906 ± 5.743 μm) mice ($p = 0.001$) and the long diameter between db/db (36.568 ± 12.230 μm) and control (31.015 ± 7.228 μm) mice ($p < 0.001$). However, their heights were almost similar (8.586 ± 3.763 μm in db/db and 8.442 ± 2.323 μm in control mice, $p < 0.695$). Some db/db mice had a long diameter > 80 μm (Figure 5F).

3.4 | Change in SMA cross-sectional area according to db/db-mice age

Figure 6A demonstrates that cross-sectional area increased with age (control: 221.782 ± 121.230 μm; 14 weeks: 294.378 ± 151.008 μm; and 28 weeks: 312.925 ± 147.943 μm) in the analysis of nonsliced SMAs. Significant differences were noted between the control and 14-week mice ($p < 0.001$) as well as between the control and 28-week mice ($p < 0.001$) but not between the 14- and 28-week mice (p value = 0.772). In sliced SMAs (Figure 6B), the short and long diameters increased significantly with age (short diameters: 21.906 ± 5.743 μm in control mice, 23.505 ± 5.283 μm in 14-week db/db mice, and 25.476 ± 4.913 μm in 28-week db/db/ mice; long diameters: 31.015 ± 7.228 μm in control mice, 35.062 ± 11.29 μm in 14-week db/db mice, and 36.568 ± 12.229 μm in 28-week db/db/ mice). Between the two groups, all differences were significant (all $p < 0.005$), except that between the 14- and 28-week mice with regard to the long diameter ($p = 0.660$). There was no significant difference in SMA height between the two groups ($p = 0.165$).

4 | DISCUSSION

The cochlear artery, a branch of the labyrinthine artery from the anterior inferior cerebellar artery, is the primary source of blood to the cochlea. Due to blood-pressure dysregulation of the stria vascularis in the cochlea, hearing loss is aggravated by small-vessel diseases, such as age, hypertension, diabetes, coronary heart disease, or cerebral ischemia.[11] Ohlemiller et al. reported that the number of inner and outer hair cells progressively reduced following hypoperfusion of the cochlea due to atherosclerosis, predominantly at the basal turn.[12] In a previous study, vascular insufficiency was found to be the primary cause of acute hearing loss. We demonstrated that dilatation or deviation of the vertebrobasilar artery induces sudden hearing loss.[13] The close relationship of plasma fibrinogen[14] or neutrophil-to-lymphocyte ratio[15] with hearing loss potentially constitutes evidence for considering increased blood viscosity or vascular insufficiency as factors that aggravate hearing loss. We hypothesized that DM-related hearing loss is potentially predominantly caused by small-vessel disease. In this

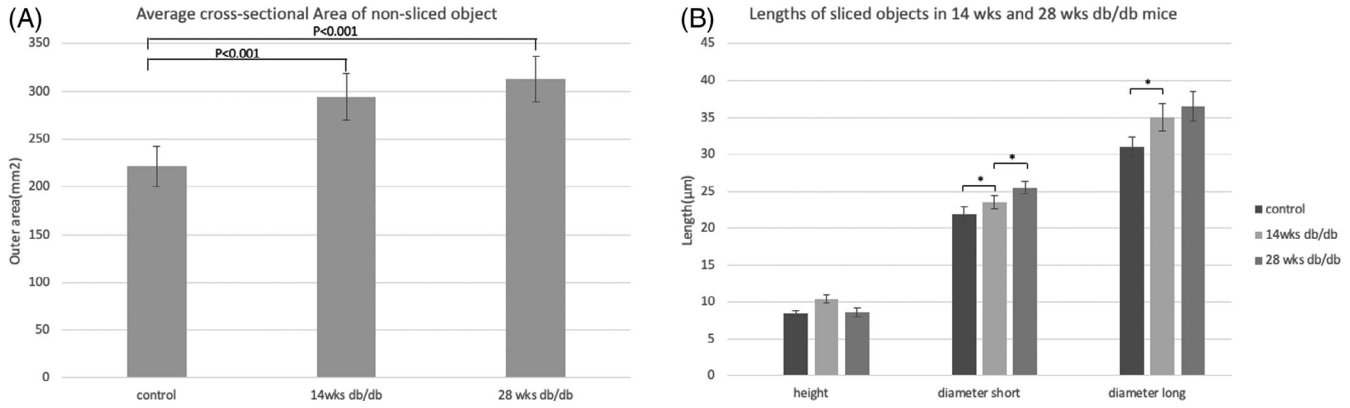

FIGURE 6 Changes in SMA cross-sectional area according to age (14 and 28 weeks) of db/db mice. (A) Graph comparing SMA cross-sectional area (outer area) in nonsliced objects. (B) Graph comparing the height, shortest diameters, and longest diameters of the SMA in sliced objects. The lengths of the bars and mean ± SEs of the values. * means $p < 0.005$.

study, we found that db/db mice had thicker and larger proximal-SMA vessel walls and diameters than control mice, respectively. Arterial resistance is usually determined by the presence of thick muscular walls and a narrow lumen and contributes the most to blood-flow resistance.[16] Consequently, chronic high resistance in the vessel causes it to enlarge.[17]

Although a direct causal relationship between type 2 diabetes with inner-ear pathology and accompanying hearing loss has been difficult to prove, a recent review revealed that hearing loss is approximately twice as common in adults with diabetes compared with that in those without the disease, and those with prediabetes have a 30% higher rate of hearing loss.[4] Cerebral small-vessel disease is common in neurologically asymptomatic individuals with type 1 diabetes.[18] The retinal vasculature is thought to mirror the brain vasculature; however, data on this association in type 1 diabetes are limited.[19] Recent studies have revealed that carotid intima-media thickness is associated with the extent of atherosclerosis and end-organ damage and that increased carotid intima-media thickness is related to hearing disorders in the general adult population. Endothelial dysfunction is one of the principal factors closely associated with atherosclerosis development in both type 1 and type 2 DM.[20] In a cadaver study, Kariya et al. examined whether pathological findings were present in the SMA of the cochlear vessels in patients with DM. They found that patients with type 2 DM who received insulin therapy exhibited an increased vessel-wall thickness and vessel-wall ratio compared with those with type 1 DM and concluded that the cochlea in patients with DM demonstrated circulatory disturbance compared with that in age-matched normal controls. The cadaver study was potentially limited by ignorance of several uncontrolled cofactors that affect vessel size and vessel changes after death. Even though we did not measure the hearing in mice, we supposed that the pathophysiologic change would occur prior to the deterioration of hearing. Therefore, we intended to confirm these pathologic changes in a well-controlled animal study involving 3D-analyzed quantifications, such as vessel thickness, short and long diameters of cross-sectioned vessels, and volume of vessels.

The db/db-mouse model of leptin deficiency is currently the most widely used mouse model for type 2 DM.[21] A previous study demonstrated that leptin-deficient db/db mice potentially display microvascular dysfunction in both the coronary and renal vascular beds.[22] Therefore, this model may be suitable for translational, mechanistic, and interventional studies to improve our understanding of microvascular complications in type 2 diabetes. Leptin may target the labyrinth and contribute to the ongoing protection of the inner ear.[23] Leptin disturbances potentially contribute to metabolic syndromes involving the audiovestibular system. Another study on the relationship between leptin and hearing loss revealed that serum leptin levels in patients with idiopathic sudden sensorineural hearing loss did not differ from those in controls.[24] We did not measure leptin levels in mice; however, leptin-deficient db/db mice were affected by thick vessel walls, enlarged vessels, and microvascular disturbances of the SMA in the cochlea. Compensatory arterial enlargement is a pathological response to early atherosclerosis.[17] Human arteries are dynamic conduits that respond to different stimuli by remodeling their structure and size. All peripheral arteries dilate in response to intima-media thickening and early atherosclerotic plaque formation. The percentage increase in the external diameter was significantly related to lesion thickness. A similar correlation has recently been reported between plaque volume and total arterial cross-sectional area in coronary arteries studied using intravascular ultrasound.[25] The mechanism of compensatory enlargement requires further study in the future.

Vessel size (diameter) in biological systems is routinely evaluated using large image stacks acquired using conventional microscopy with histological sections. Even though conventional histology provides favorable spatial resolution for evaluating microvascular structure, it cannot produce 3D information without exact perpendicular sections according to the longitudinal axis of the vessels. This limitation could lead to misinterpretation of complex microvessel configurations in health and disease. However, laser scanning microscopy (LSM) is a nondestructive method that produces well-registered optical sections suitable for the 3D reconstruction of vessels and can be processed without any histological sectioning. It is necessary to visualize and assess all SMA maps from high to low, that is, from the cochlear base to the apex. We selected the section of the 3D SMA from the base to

the middle turn because the peripheral portions of the SMA are considerably small and varied, thus affecting average SMA-diameter results. Current efforts are underway to include the use of automated segmentation and machine-learning processes to facilitate automated interpretation and improve quality-control measures.[26] In our study, 3D-rendered structures of SMAs autocalculated by Arivis Vision4D volume analysis were used to visualize the 3D anatomy of microvessels.

5 | CONCLUSION

The SMA, as the main cochlear artery, is an important factor in aggravating diseases related to hearing loss. Using the 3D reconstruction technique by LSM in the cochlea, we found that db/db mice had thicker proximal-SMA vessel walls and larger vessel diameters in the 3D quantitative analysis compared with that of the control mice. The cochlea in patients with DM potentially demonstrated circulatory disturbance compared with that in age-matched normal controls because of the high DM-related arterial resistance associated with thick muscular walls and a narrow lumen. Based on this pathologic evidence, healthy diets and the adoption of a healthy lifestyle, in general, have been suggested to prevent the progression of both diabetes and hearing loss.

ORCID

Young Joon Seo https://orcid.org/0000-0002-2839-4676
Dae Bo Shim https://orcid.org/0000-0002-2331-5000
Ryu Takechi https://orcid.org/0000-0001-6359-3382
Daniel Brown https://orcid.org/0000-0001-6097-637X

REFERENCES

1. Ahn Y, Seo YJ, Lee YS. The effectiveness of hyperbaric oxygen therapy in severe idiopathic sudden sensorineural hearing loss. *J Int Adv Otol*. 2021;17(3):215-220.
2. Shi X. Physiopathology of the cochlear microcirculation. *Hear Res*. 2011;282(1–2):10-24.
3. Shi X, Zhang F, Urdang Z, et al. Thin and open vessel windows for intra-vital fluorescence imaging of murine cochlear blood flow. *Hear Res*. 2014;313:38-46.
4. Samocha-Bonet D, Wu B, Ryugo DK. Diabetes mellitus and hearing loss: a review. *Ageing Res Rev*. 2021;71:101423.
5. Curhan SG, Wang M, Eavey RD, Stampfer MJ, Curhan GC. Adherence to healthful dietary patterns is associated with lower risk of hearing loss in women. *J Nutr*. 2018;148(6):944-951.
6. Kariya S, Cureoglu S, Fukushima H, et al. Comparing the cochlear spiral modiolar artery in type-1 and type-2 diabetes mellitus: a human temporal bone study. *Acta Med Okayama*. 2010;64(6):375-383.
7. Wua J, Wang HM, Li J, Men XL. The research applications of db/db mouse. *Sheng Li Ke Xue Jin Zhan*. 2013;44(1):12-18.
8. Li J, Wang JJ, Yu Q, Wang M, Zhang SX. Endoplasmic reticulum stress is implicated in retinal inflammation and diabetic retinopathy. *FEBS Lett*. 2009;583(9):1521-1527.
9. Santi PA. Light sheet fluorescence microscopy: a review. *J Histochem Cytochem*. 2011;59(2):129-138.
10. Brown DJ, Pastras CJ, Curthoys IS, Southwell CS, Roon LV. Endolymph movement visualized with light sheet fluorescence microscopy in an acute hydrops model. *Hear Res*. 2016;339:112-124.
11. Agrawal Y, Platz EA, Niparko JK. Risk factors for hearing loss in US adults: data from the National Health and nutrition examination survey, 1999 to 2002. *Otol Neurotol*. 2009;30(2):139-145.
12. Ohlemiller KK, Gagnon PM. Cellular correlates of progressive hearing loss in 129S6/SvEv mice. *J Comp Neurol*. 2004;469(3):377-390.
13. Han SM, Lee HS, Chae HS, Seo YJ. Usefulness of vertebrobasilar artery radiological finding as a predictive and prognostic factor for sudden sensorineural hearing loss. *Auris Nasus Larynx*. 2021;48(5):823-829.
14. Park YAH, Kong TH, Seo YJ. A sustained increase of plasma fibrinogen in sudden sensorineural hearing loss predicts worse outcome independently. *Am J Otolaryng*. 2017;38(4):484-487.
15. Seo YJ, Jeong JH, Choi JY, Moon IS. Neutrophil-to-lymphocyte ratio and platelet-to-lymphocyte ratio: novel markers for diagnosis and prognosis in patients with idiopathic sudden sensorineural hearing loss. *Dis Markers*. 2014;2014:702807.
16. Gomez-Lara J, Teruel L, Homs S, et al. Lumen enlargement of the coronary segments located distal to chronic total occlusions successfully treated with drug-eluting stents at follow-up. *EuroIntervention*. 2014;9(10):1181-1188.
17. Shimokawahara H, Ogawa A, Mizoguchi H, Yagi H, Ikemiyagi H, Matsubara H. Vessel stretching is a cause of lumen enlargement immediately after balloon pulmonary angioplasty: intravascular ultrasound analysis in patients with chronic thromboembolic pulmonary hypertension. *Circ Cardiovasc Interv*. 2018;11(4):e006010.
18. Eriksson MI, Summanen P, Gordin D, et al. Cerebral small-vessel disease is associated with the severity of diabetic retinopathy in type 1 diabetes. *BMJ Open Diabetes Res Care*. 2021;9(1):e002274.
19. Liew G, Gopinath B, White AJ, Burlutsky G, Wong TY, Mitchell P. Retinal vasculature fractal and stroke mortality. *Stroke*. 2021;52(4):1276-1282.
20. Chakir M, Plante GE. Endothelial dysfunction in diabetes mellitus. *Prostaglandins Leukot Essent Fatty Acids*. 1996;54(1):45-51.
21. Alpers CE, Hudkins KL. Mouse models of diabetic nephropathy. *Curr Opin Nephrol Hypertens*. 2011;20(3):278-284.
22. Westergren HU, Grönros J, Heinonen SE, et al. Impaired coronary and renal vascular function in spontaneously type 2 diabetic leptin-deficient mice. *PLoS One*. 2015;10(6):e0130648.
23. Horner KC, Troadec JD, Blanchard MP, Dallaporta M, Pio J. Receptors for leptin in the otic labyrinth and the cochlear–vestibular nerve of Guinea pig are modified in hormone-induced anorexia. *Hear Res*. 2010;270(1–2):48-55.
24. Ural A, Alver A, Isik AU, Imamoglu M. Serum leptin levels in patients with idiopathic sudden sensorineural hearing loss. *J Int Adv Otol*. 2015;10(3):201-204.
25. Nicholls SJ, Tuzcu EM, Wolski K, et al. Extent of coronary atherosclerosis and arterial remodelling in women: the NHLBI-sponsored Women's ischemia syndrome evaluation. *Cardiovasc Diagn Ther*. 2018;8(4):405-413.
26. Eskandari M, Kramer CM, Hecht HS, Jaber WA, Marwick TH. Evidence base for quality control activities in cardiovascular imaging. *JACC Cardiovasc Imaging*. 2016;9(3):294-305.

How to cite this article: Seo YJ, Shim DB, Sharif A, Samson Z, Takechi R, Brown D. Circulatory disturbance of the cochlear spiral modiolar artery in a type 2 diabetic mouse model. *Laryngoscope Investigative Otolaryngology*. 2022;7(5):1568-1574. doi:10.1002/lio2.917